Mon. Not. R. Astron. Soc. **371,** 19–28 (2006) doi:10.1111/j.1365-2966.2006.10610.x

V0332+53 in the outburst of 2004–2005: luminosity dependence of the cyclotron line and pulse profile

S. S. Tsygankov,[1,2]★ A. A. Lutovinov,[1,2] E. M. Churazov[1,2] and R. A. Sunyaev[1,2]

[1]*Space Research Institute, Profsoyuznaya str. 84/32, Moscow 117997, Russia*
[2]*MPI for Astrophysik, Karl-Schwarzschild str. 1, Garching 85741, Germany*

Accepted 2006 May 24. Received 2006 May 23; in original form 2005 November 15

ABSTRACT

We present the results of observations of the transient X-ray pulsar V0332+53 performed during a very powerful outburst, from 2004 December to 2005 February, with the *INTEGRAL* and *RXTE* observatories in a wide (3–100 keV) energy band. A cyclotron resonance scattering line at an energy of ∼26 keV has been detected in the source spectrum together with its two higher harmonics at ∼50 and ∼73 keV, respectively. We show that the energy of the line is not constant but changes linearly with the source luminosity. Strong pulse profile variations, especially near the cyclotron line, are revealed for different levels of source intensity. We discuss the obtained results in terms of the theoretical models of X-ray pulsars.

Key words: pulsars: individual: V0332+53 – X-ray: binaries.

1 INTRODUCTION

The transient X-ray pulsar V0332+53 was discovered by the Vela 5B observatory in 1973 (Terrel & Predhorsky 1973) during an outburst when its intensity reached ∼1.4 Crab in the 3–12 keV energy band. The outburst lasted about three months before the source became undetectable again.

During observations in 1983 November to 1984 January, the pulsar's and orbital parameters were determined with the *EXOSAT* observatory: the pulse period was determined to be ∼4.375 s, the orbital period 34.25 d, eccentricity 0.31 and the projected semimajor axis of the neutron star $a_x \sin i \simeq 48$ lt-s (Stella et al. 1985). These authors also mentioned that as the source intensity decreased, the pulse profile changed from double to single peaked, which was accompanied by significant hardening of the source spectrum. Later, when the source was observed by the *Ginga* observatory the cyclotron resonance scattering feature with an energy of $E_{\rm cyc} = 28.5 \pm 0.5$ keV was detected in its spectrum. This energy corresponds to a magnetic field on the neutron star surface of $\sim 3 \times 10^{12}$ G (Makishima et al. 1990). Later, Mihara et al. (1998) reported measurements of two different values of the resonance energy for different levels of the source intensity.

The next powerful outburst of the source began at the end of 2004 (Swank, Remillard & Smith 2004). This outburst had been predicted on the basis of the increasing optical brightness of the normal companion, which reached its maximum on 2004 January 31 (Goranskij & Barsukova 2004). A preliminary analysis of *RXTE* observations performed during 2004 December 24–26 showed that besides the absorption feature at an energy of 26.34 ± 0.03 keV, there are two additional similar features in the source spectrum at energies of 49.1 ± 0.2 and 74 ± 2 keV. These features were interpreted as the second and third harmonics of the main cyclotron frequency (Coburn et al. 2005). Similar results were inferred from the analysis of the first ∼100 ks data of the *INTEGRAL* observatory (Kreykenbohm et al. 2005).

Negueruela et al. (1999) discussed the results of the optical observations of BQ Cam – the normal companion of the X-ray pulsar V0332+53. They determined the star's spectral class as O8-9Ve and estimated the distance to the system at ∼7 kpc.

In this paper, we present the results of an analysis of observations of V0332+53 performed with the *INTEGRAL* and *RXTE* observatories in 2005 January to February. Our main aim is to study variations of the source spectrum and pulse profile depending on its intensity. Results of the analysis based on *RXTE* data and independent analysis of the *INTEGRAL* data can be found in Pottschmidt et al. (2005) and Mowlavi et al. (2006), respectively. The observations, instruments and data analysis are described in Section 2. In Section 3, we demonstrate for the first time that the energy of the cyclotron resonance scattering feature is not constant but linearly increases with decreasing luminosity of the source. Section 4 is dedicated to a detailed study of the pulse profile variations especially near the cyclotron line. The obtained results are discussed in Section 5.

2 OBSERVATIONS AND DATA ANALYSIS

The X-ray pulsar V0332+53 was observed several times with the *INTEGRAL* and *RXTE* observatories during the end of 2004 and the beginning of 2005. About 130 pointed observations were carried out by the *INTEGRAL* observatory (Winkler et al. 2003) during target of opportunity (TOO) observations of the source with a total exposure

★E-mail: st@hea.iki.rssi.ru (SST)

time of ∼400 ks. (These data are publicly available.) Data of the IBIS telescope [the *INTEGRAL* Soft Gamma-Ray Imager (ISGRI) detector; Lebrun et al. 2003] and Joint European X-ray Monitor (JEM-X) (Lund et al. 2003) were used in the analysis. The effective energy bands of these instruments are 20–200 and 3–30 keV, respectively, which makes it possible to study bright astrophysical objects in a wide energy band.

The image reconstruction was done with the method and software described in Revnivtsev et al. (2004). The source spectra in a hard energy band (>20 keV) obtained by the IBIS telescope were calculated through the reconstruction of a large number of images of the source in narrow energy channels and flux extraction of the studied source. The response matrix for our research has been done based on the standard *INTEGRAL* matrix (taken from the OSA package), but the new arf-file was calculated using the calibration observations of the Crab nebulae. Standard calibration tables and procedures (similar to those implemented in OSA 5.0) were used to correct the energy of ISGRI events having different rise time. The analysis of a large number of calibration observations for the Crab nebula revealed that this method has a systematic error in measuring source fluxes of about ∼3 per cent. We included this systematic uncertainty when analysing spectra with the XSPEC package.

For the timing analysis on time-scales of the order of the source pulse period and for the analysis of the JEM-X data, we used the standard OSA 5.0 software package provided by the *INTEGRAL* Science Data Center (http://isdc.unige.ch). For the pulse profile reconstruction at high energies, the first three steps of OSA (COR, GTI, DEAD) were executed. After this, we collected photons with specified energies from the detector pixels opened for the source using the tool EVTS_EXTRACT. At the next stage, the arrival times of collected photons were corrected for the neutron star orbital motion using the known binary parameters (Stella et al. 1985). Such a relatively simple approach for collecting photons is justifiable in our case as the source V0332+53 was a single object in the telescope field of view. Thus, the detector collects only photons from the source and background photons. The background can be calculated from those pixels which are fully closed for the source by the opaque mask elements. To reconstruct the pulse profile at low energies (JEM-X data), photons from the whole detector were collected (the tool EVTS_PICK). The subsequent timing analysis was done with the FTOOLS package.

Due to a nicety of the considering effects (in particular a displacement of the cyclotron line centre is about ∼3 keV in the *INTEGRAL* data) and the use of different types of the software on different stages of the analysis, we carried out an additional investigation of accuracy and stability of the energy determination for both types of the software. The tungsten K_α line 59.32 keV was chosen as a calibration line due to its brightness. (Strictly speaking, in this spectral region there is a blend of tungsten lines at energies 57.98, 59.32, etc. keV, but line at 59.32 keV is the most strong one.) The detector spectrum was built for both the software (For OSA 5.0 it was done after the DEAD level.), then the energy of the line centre was determined and compared with ones from other observations and its theoretical value. It was shown that the line centre position is stable and in good agreement with the theoretical one in the spectral analysis [Fig. 1(a)]. The conservative estimation of the systematic uncertainty of the energy determination gives ∼0.1 keV.

For the standard software OSA 5.0, the line centre position is changed from one observation to another and displaced from the theoretical value [Fig. 1(b)]. Therefore in the following analysis, we took it into account and made a correction for this effect.

Apart from *INTEGRAL* data, we also used data of the *RXTE* observatory (Bradt, Rothschild & Swank 1993): simultaneous data of the all-sky monitor (ASM) (http://xte.mit.edu/ASM_lc.html), and the spectrometers Proportional Counter Array (PCA) and High Energy X-ray Timing Experiment (HEXTE) (Obs. ID 90427), operating in the energy bands 1.3–12.2, 3–20 and 15–250 keV, respectively. For the *RXTE* data reduction, we used standard programs of FTOOLS/LHEASOFT 5.3 package. As for the ISGRI detector, we investigated the accuracy of the energy determination using the HEXTE spectrometer. In this analysis, we used the ^{241}Am calibration line at 59.6 keV. To estimate the systematic error of energy measuring, we determined a typical scatter of measurements of the line centre, ∼0.1 keV. This value was added as a systematic error to the uncertainties obtained from the spectral analysis.

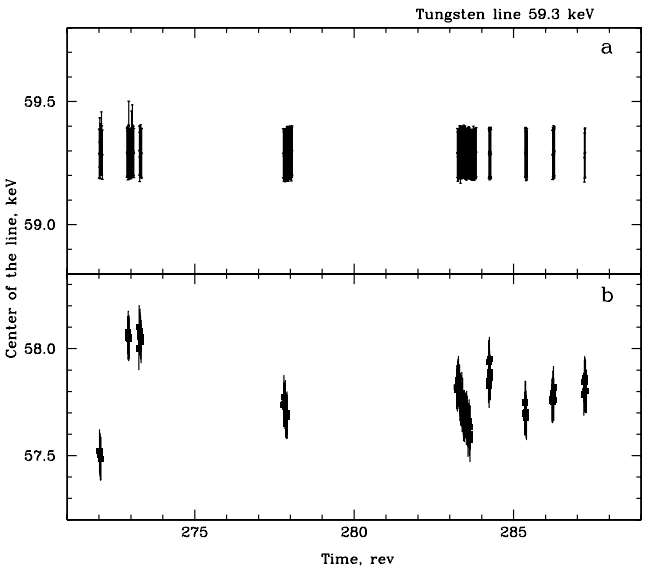

Figure 1. Dependence of the energy of the tungsten line 59.3 keV, measured by the ISGRI detector, from the observation date for special (a) and standard OSA 5.0 (b) software.

A list of observations of the X-ray pulsar V0332+53 is presented in Table 1. The date of observations, corresponding exposure, observed source flux and luminosity are given. Luminosity was calculated assuming a source distance of 7 kpc. The obtained luminosity values may be regarded as close to the bolometric ones on the assumption that the bulk of the energy is released in X-rays.

3 LIGHT CURVES

The daily-averaged light curve of the X-ray pulsar V0332+53 obtained by ASM/*RXTE* is presented in Fig. 2(a). The source intensity was increasing practically linearly for ∼30 d, then the source stayed for about 10 d near the maximum of its intensity and after that the measured flux decreased to the pre-outburst value in ∼50 d. The last segment of the light curve can be described by an exponential decay with a characteristic time of $\tau \sim 17$ d. A comparison of the 2004–2005 outburst with previous type II outbursts (Stella, White & Rosner 1986) shows that it is a typical outburst of this class for V0332+53 in terms of duration and maximum of X-ray flux.

INTEGRAL observations started only several days after the outburst maximum due to the limitations of the satellite orientation relative to the Sun. In Fig. 2(b), the pulsar light curve obtained by the ISGRI detector in the hard (18–60 keV) energy band is shown. Each point corresponds to a separate observation with exposure of about 2 ks. The figure demonstrates that the source flux in hard

Table 1. Observations of the X-ray pulsar V0332+53 with the *INTEGRAL* and *RXTE* observatories in 2004–2005.

Date, MJD (rev)	Exposure (ks)	Flux[a] ($\times 10^{-9}$ erg s^{-1} cm^{-2})	Luminosity[b] (10^{37} erg s^{-1})
	INTEGRAL data		
53376.5 (272)	28.7	58.3 ± 0.9	34.1 ± 0.5
53379.2 (273)	56.7	45.6 ± 0.4	26.7 ± 0.2
53380.3 (274)	21.1	40.7 ± 2.4	23.8 ± 1.4
53394.0 (278)	72.3	24.9 ± 1.0	14.5 ± 0.6
53410.9 (284)	149.1	12.5 ± 0.2	7.3 ± 0.1
53413.1 (285)	15.5	11.4 ± 0.3	6.7 ± 0.2
53416.5 (286)	15.4	8.4 ± 0.3	4.9 ± 0.2
53419.1 (287)	17.0	7.0 ± 0.3	3.4 ± 0.2
53422.1 (288)	20.1	3.5 ± 0.2	2.0 ± 0.1
	RXTE data		
53367.2 (90427-01-01-00G)	1.5	82.4 ± 2.0	48.4 ± 1.2
53368.3 (90427-01-01-01)	2.2	81.6 ± 2.4	48.0 ± 1.4
53368.9 (90427-01-01-02)	1.8	79.2 ± 0.5	46.7 ± 0.3
53369.6 (90427-01-01-03)	1.9	72.9 ± 0.4	42.9 ± 0.2
53374.0 (90427-01-02-00)	0.9	68.5 ± 2.1	40.3 ± 1.2
53375.0 (90427-01-02-01)	0.8	60.9 ± 2.1	35.8 ± 1.2
53376.3 (90427-01-02-02)	0.7	66.0 ± 2.6	38.8 ± 1.5
53376.7 (90427-01-02-03)	2.7	61.9 ± 1.3	36.4 ± 0.8
53385.1 (90427-01-03-01)	9.9	43.7 ± 1.5	25.7 ± 0.9
53385.5 (90427-01-03-02)	14.5	41.5 ± 0.2	24.4 ± 0.1
53387.0 (90427-01-03-05)	12.8	38.0 ± 0.1	22.3 ± 0.1
53387.4 (90427-01-03-06)	12.1	36.5 ± 0.1	21.5 ± 0.1
53387.9 (90427-01-03-07)	9.6	37.2 ± 0.1	21.9 ± 0.1
53388.4 (90427-01-03-09)	11.9	34.5 ± 0.8	20.3 ± 0.5
53389.0 (90427-01-03-11)	9.9	34.5 ± 0.4	20.3 ± 0.2
53389.3 (90427-01-03-12)	9.7	34.1 ± 1.0	20.1 ± 0.6
53413.1 (90427-01-04-00)	6.1	14.7 ± 0.6	8.6 ± 0.3
53413.8 (90427-01-04-04)	6.7	12.6 ± 0.4	7.4 ± 0.2
53414.3 (90427-01-04-02)	11.8	11.1 ± 0.2	6.5 ± 0.1
53414.5 (90427-01-04-03)	6.8	11.0 ± 0.3	6.5 ± 0.2
53414.8 (90427-01-04-05)	2.6	10.9 ± 0.2	6.4 ± 0.1
53416.6 (90427-01-04-01)	5.7	8.9 ± 0.2	5.2 ± 0.1

[a]In the 3–100 keV energy band.
[b]In the 3–100 keV energy band, assuming source distance of 7 kpc.

X-rays decreased from ∼900 to ∼100 mCrab during a month and a half. Note that the shape of the light curve in hard X-rays is slightly different from the one in the soft 1.3–12.2 keV energy band.

From the analysis of the V0332+53 light curve in the soft energy band, it was found that the source intensity demonstrates variability with an amplitude of about 20 per cent (near the outburst maximum). The variability amplitude decreased when the source flux decreased and practically disappeared by the end of the outburst. The variability with the same amplitude was observed with the ISGRI detector in the hard energy band too. The 18–60 keV source light curve with time resolution of 300 s is shown in Fig. 2(c) for the bright state of the source, when the variability is most visible. In the right-hand part of the figure, a local outburst with maximum at MJD 53380.3 and total duration of about 4.5 hs is seen. The solid line represents the best-fitting approximation by a Gaussian.

4 SPECTRAL ANALYSIS

The V0332+53 spectrum deserves special attention. This is only the second X-ray accreting pulsar (after 4U0115+63) whose spectrum exhibits not only a cyclotron resonance scattering feature but also its two higher harmonics (Coburn et al. 2005; Kreykenbohm et al. 2005; Pottschmidt et al. 2005). As a whole, the spectrum of the pulsar can be well described by a power law with an exponential cut-off at high energies, typical for this class of objects.

The significant number of V0332+53 observations carried out with the *INTEGRAL* and *RXTE* observatories allowed us to reconstruct the source spectrum at different phases of the outburst and to trace the evolution of its parameters. We approximated the obtained spectra with a power-law model with an exponential cut-off (cutoffpl in XSPEC), modified by three absorption lines in the form

$$\exp\left[\frac{-\tau_{\rm cycl}(E/E_{\rm cycl})^2\sigma_{\rm cycl}^2}{(E-E_{\rm cycl})^2+\sigma_{\rm cycl}^2}\right],$$

where $E_{\rm cycl}$, $\sigma_{\rm cycl}$ and $\tau_{\rm cycl}$ are the centre, width and depth of the line, respectively (Mihara et al. 1990). This model describes the source spectrum similarly well as the usual model of a power law with a high-energy cut-off (powerlaw × highecut in XSPEC; White, Swank & Holt 1983) but has fewer parameters. The best-fitting value of the cut-off energy $E_{\rm cut}$ for the powerlaw × highecut model is about 5–6 keV. Given the limited energy range of the used instruments (down to 3 keV for PCA and 4.5 keV for JEM-X), it is not possible to put tight constraints on the photon index. An iron emission line was

Table 2. Best-fit parameters of the spectrum of V0332+53 in the bright state.

Model parameter	Value
Photon index	-0.120 ± 0.008
$E_{\rm cut}$, keV	9.21 ± 0.04
$\tau_{\rm cycl,1}$	1.91 ± 0.02
$E_{\rm cycl,1}$, keV	$25.92^{+0.07}_{-0.08}$
$\sigma_{\rm cycl,1}$, keV	$5.44^{+0.08}_{-0.06}$
$\tau_{\rm cycl,2}$	2.12 ± 0.03
$E_{\rm cycl,2}$, keV	$49.44^{+0.07}_{-0.14}$
$\sigma_{\rm cycl,2}$, keV	$9.89^{+0.20}_{-0.23}$
$\tau_{\rm cycl,3}$	1.26 ± 0.10
$E_{\rm cycl,3}$, keV	$72.1^{+0.5}_{-0.6}$
$\sigma_{\rm cycl,3}$, keV	$10.1^{+0.5}_{-0.9}$
χ^2 (d.o.f)	1.25 (136)

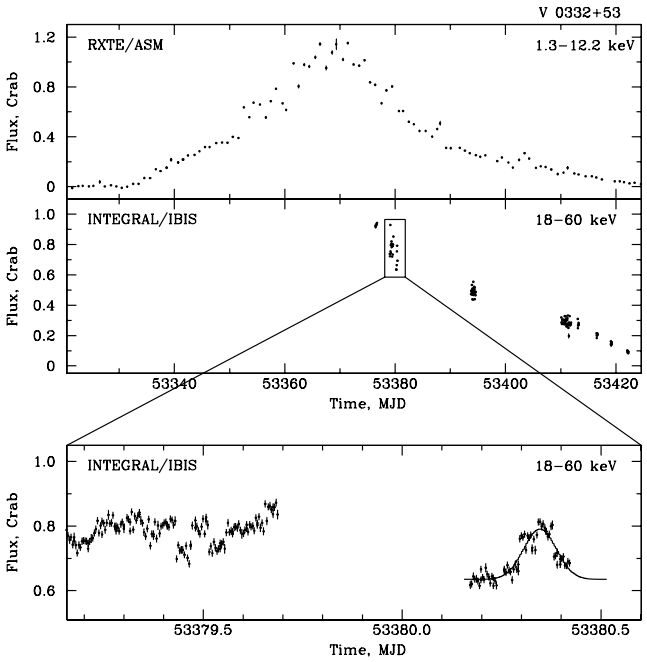

Figure 2. Light curves of the X-ray pulsar V0332+53 obtained during the outburst: (a) with the ASM/*RXTE* monitor; (b) with the IBIS/*INTEGRAL* telescope in a hard energy band and (c) with the IBIS/*INTEGRAL* telescope with a time resolution of 300 s for the bright state. Solid line represents the best-fitting approximation of the small outburst by a Gaussian with maximum at MJD 53380.3 and total width of ∼4.5 h.

added to the model when fitting the *RXTE* data. This feature is not detected by the JEM-X monitor partly due to its lower sensitivity compared to PCA, and also due to the current uncertainty in the JEM-X response matrix at these energies. [See comments in Filippova et al. (2005) for details.]

A typical source spectrum obtained with the *INTEGRAL* observatory for the bright (272 rev) state is shown in Fig. 3. The best-fitting parameters are summarized in Table 2.

For comparison, the spectrum obtained in the low state (284 rev) is shown in the same figure.

The cyclotron resonance scattering feature and its second harmonic are clearly visible in both spectra. Despite the rapid decrease in the source intensity and its weakness at high energies (>65 keV), inclusion into the model of the third harmonic with an energy of

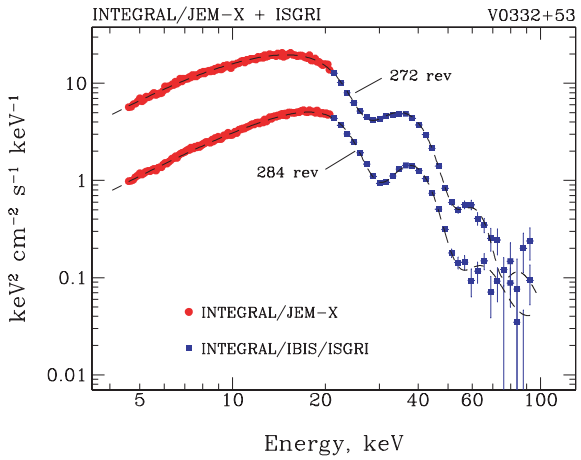

Figure 3. Energy spectra of V0332+53 measured with the *INTEGRAL* observatory for two states (272 and 284 rev).

∼75–80 keV leads to a significant improvement in the fit [$\Delta\chi^2 = 18$ for 3 degrees of freedom (d.o.f.)]. This harmonic is also detected in several other observations, but its parameters (width and depth) are reasonably bounded only in the bright state (till 284 rev). Fixing them at the values obtained for the bright state does not allow one to improve the quality of the fit for the low-state spectra. Moreover, the determined linewidths for these observations are too large and strongly affect the determination of the parameters of the second harmonic, making this task model-dependent. It is necessary to note that the fundamental line energy does not depend on including the third harmonic in the model. Pottschmidt et al. (2005) used a Gaussian profile for describing the cyclotron line, and therefore obtained values of the cyclotron energy differ slightly from that of ours. The same situation was discussed by Nakajima et al. (2006) for 4U0115+634.

Our analysis showed that the model described approximates the source spectrum well during the whole outburst both for *INTEGRAL* and for *RXTE* data. The behaviour of the cyclotron line is of greatest interest because it is confidently detected during the entire outburst, and its parameters are model independent. The line energy dependence on the source luminosity obtained from *INTEGRAL* and *RXTE* data is shown in Fig. 4 by dark triangles and squares, respectively. The uncertainties of the HEXTE results are slightly higher than those for ISGRI as the HEXTE exposures are shorter (see Table 1). The measurements of both observatories are in good mutual agreement and fall on a straight line, i.e. the cyclotron line energy increases linearly with decreasing source luminosity. The formal fitting of this dependence with a linear relation gives $E_{\rm cycl,1} \simeq -0.10L_{37} + 28.97$ keV, where L_{37} is the luminosity in units of 10^{37} erg s^{-1}. Believing that for low luminosities the emission come practically from the neutron star surface (see Section 6.1), we can estimate the magnetic field on the surface

$$B_{\rm NS} = \frac{1}{\sqrt{1-\frac{2GM_{\rm NS}}{R_{\rm NS}c^2}}}\frac{28.97}{11.6} \simeq 3.0\times10^{12}{\rm G},$$

where $R_{\rm NS}$ and $M_{\rm NS}$ are the neutron star radius and mass, respectively.

As was mentioned above, the energy of the second harmonics is not reasonably determined for all observations and depends on the inclusion of the third harmonic in the model. To avoid possible contamination by this component in determining the parameters of

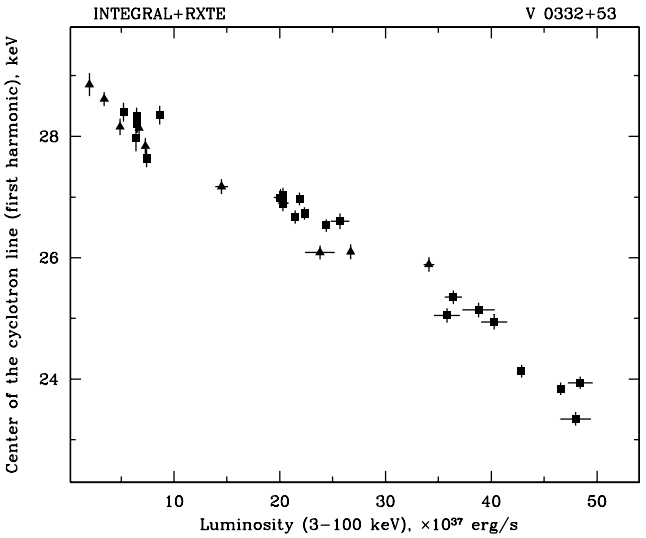

Figure 4. The cyclotron line energy dependence on the source luminosity (3–100 keV). Triangles are *INTEGRAL* results and squares are *RXTE* results.

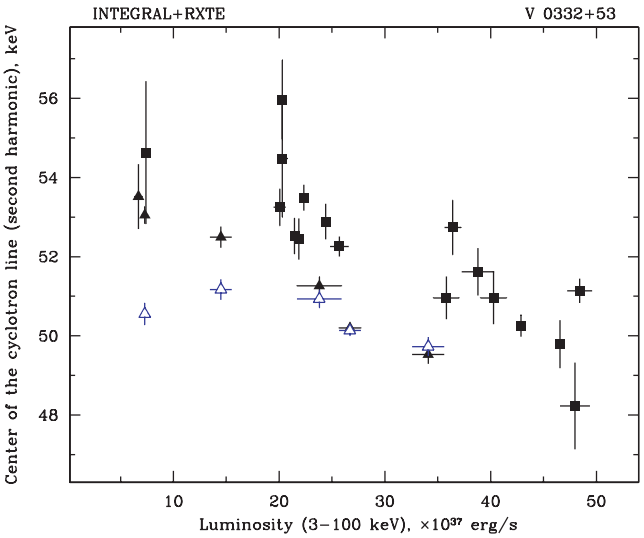

Figure 5. Same as in Fig. 4 but for the second harmonic. Open triangles represent *INTEGRAL* measurements for the broad energy band (till 110 keV) with the inclusion of the third harmonic (see text).

the second harmonic, we restricted the considered energy band by 65 keV and fitted the spectra by the same model with two absorption lines. The variation of the second harmonic with source luminosity is shown in Fig. 5 by dark triangles and squares as in Fig. 4. It can be seen that although the scatter is slightly larger than for the first harmonic, the overall tendency of the line energy increasing with decreasing luminosity holds in this case too. Formal fitting of this dependence with a linear relation gives $E_{\rm cycl,2} \propto -0.08 L_{37}$. The energy of the second harmonic was also determined by analysing the *INTEGRAL* data in the broad energy band (up to 110 keV) when the third harmonic was added to the model (open triangles in Fig. 5). The energies obtained in both analyses differ from each other, especially for the observations with low luminosities. Moreover, the ISGRI measurements lie below the near simultaneous HEXTE ones. This fact is most likely connected with the larger exposures of the ISGRI detector – its data at high energies provide better statistics and the third harmonic affect the determination of the parameters of the second harmonic even in the case of the energy band truncated at 65 keV. If we exclude the *INTEGRAL* results, then formal fitting of the HEXTE measurements results in $E_{\rm cycl,2} \propto -0.1 L_{37}$, which is the same as was obtained earlier for the main harmonic.

5 PULSE PROFILE

Because of the high intensity of the pulsar emission, we succeeded in studying its pulse profile dependence on the energy band and luminosity. As the background does not affect on the pulse profile shape, which is studied in this paper, it was not subtracted in the following analysis. The most characteristic source pulse profiles obtained with the *INTEGRAL* observatory in different energy bands are shown in Fig. 6 for two observations (272 and 284 rev). The observed peculiarities in the pulse profile behaviour can be divided in two main groups: an asymmetrical evolution of the double-peaked profile in wide energy bands and its drastic changes near the main harmonic of the cyclotron line. Below, we describe these effects in detail.

In the brightest state (272 rev), the pulse profile has a sinusoidal double-peaked shape with little prevalence of the second peak at low energies (3–6 keV). As the photon energy grows, the relative contribution of the first peak increases and exceeds the second peak intensity in the 10–15 keV energy band. The intensity of the first peak continues to grow when increasing the energy and becomes significantly larger than the second one in the 30–50 keV channel. No significant movements of the peaks depending on the energy band occur.

As the pulsar intensity diminishes, significant changes of the pulse profile occur in soft energy bands (JEM-X data): in the 3–6 keV band, it becomes nearly single-peaked in the 274 revolutions; the relative intensity of the first peak is very small in 3–6 and 6–10 keV bands in 278 and 284 revolutions. In high-energy channels (ISGRI data), the pulse profile evolves similarly as was described above for the 272 revolutions. In the following observations (beginning from the 284 revolution when the source luminosity dropped to $\sim 7.3 \times 10^{37}$ erg s^{-1}), the main described tendencies persist at soft energies, but at energies of the order and above the cyclotron one a drastic change in the pulse profile takes place: the intra-peak gap disappears and the double-peaked profile transforms into an asymmetrical single-peaked one. When the energy increases, the phase of the main minimum is displaced on the pulse phase of $\sim$0.5 (Fig. 6). The described features remain approximately the same in wide energy channels for the subsequent observations, i.e. at lower luminosities.

A detailed study of pulse profiles was carried out in narrow energy channels in the most interesting region – around the main harmonic of the cyclotron line (Fig. 7). Such a study was performed for four *INTEGRAL* observations (revolutions 272, 278, 284 and 286) and for four *RXTE* observations which are close to *INTEGRAL* ones (90427−01−02−03, 90427−01−03−11+12, 90427−01−04−00 and 90427−01−04, respectively). The last was done to obtain an independent confirmation of the *INTEGRAL* results. In Fig. 7, pulse profiles for these *INTEGRAL* observations are drawn. The energy channels were chosen to divide the cyclotron line in half, their width was approximately the same and about a half of the cyclotron linewidth (i.e. two central channels correspond to the lower and upper wings of the line). Here, we took into account that the energy of the line centre changes with the source luminosity.

For the brightest state (272 rev), the passage through the line centre does not affect the pulse profile, and all the tendencies

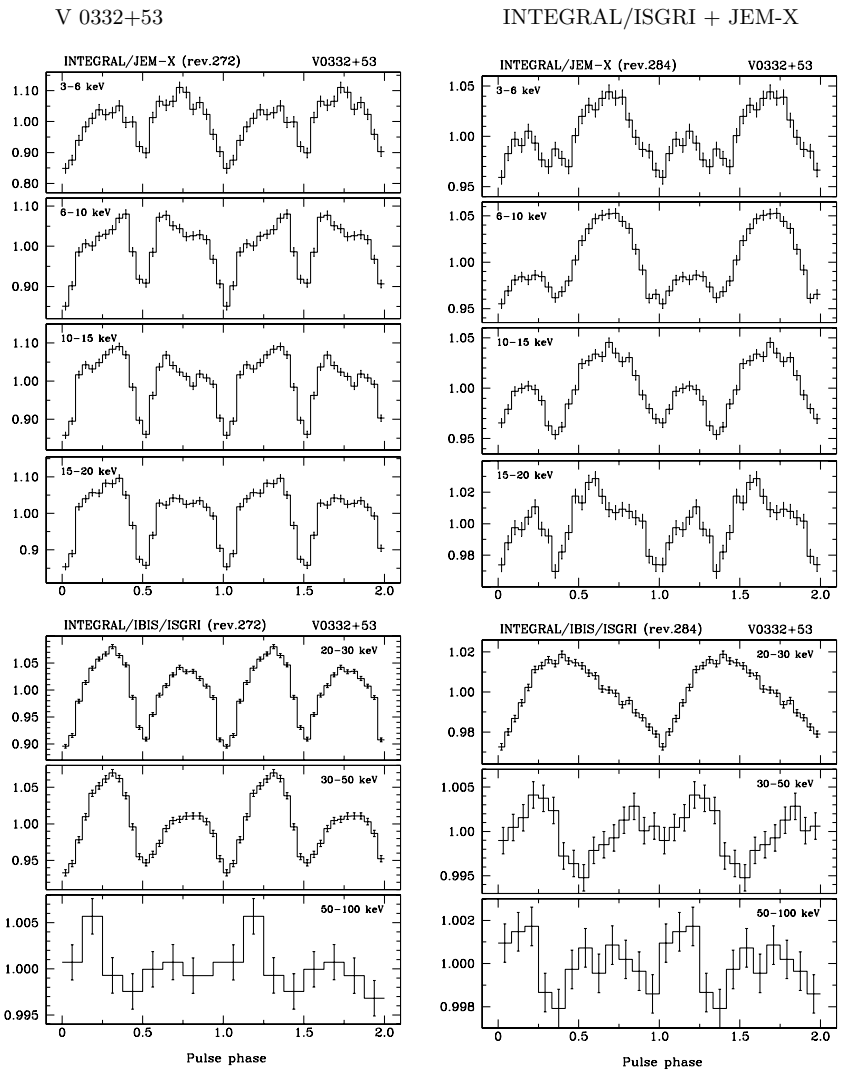

Figure 6. V0332+53 pulse profiles obtained with the JEM-X monitor and IBIS telescope of the *INTEGRAL* observatory in different energy bands for different source intensities. The pulse phase zero for each observation is chosen independently.

described above for wide channels remain. In the subsequent observations (273–278 rev), some changes occur in the relative intensity of the peaks and their positions, but the pulse profile remains double-peaked. With a further decrease in the luminosity to $\sim 7.3 \times 10^{37}\,\mathrm{erg\,s^{-1}}$ (284 rev), the profile became asymmetrical single-peaked at energies below the cyclotron line with a drastic transition to the double-peaked shape above the line energy. Unlike in the 278 revolution, the displacement of the profile by half a period, expressed in the displacement of the main minimum, occurs not in the upper wing of the line but in the next energy channel (Fig. 7). A similar picture remains when the pulsar luminosity is decreased to $\sim 4.9 \times 10^{37}\,\mathrm{erg\,s^{-1}}$ (286 rev). In the next revolution (the luminosity is $\sim 3.4 \times 10^{37}\,\mathrm{erg\,s^{-1}}$), the pulse profile at energies below the line returned to the double-peaked shape, although the single-peaked one holds in the lower wing. The displacement of the profile by half a period is retained in the last channel too. It is necessary to note that due to the source intensity decreasing the statistics in the last observations is not sufficient for detailed analysis of the pulse profile structure, and we can only consider their common characteristics.

The results of a similar analysis performed on the *RXTE*/HEXTE data (bottom panels on Fig. 7) fully confirm the conclusions about the behaviour of the pulse profile drawn above based on the *INTEGRAL*/ISGRI data.

6 DISCUSSION

The transient X-ray pulsar V0332+53 demonstrates powerful outbursts in which its intensity exceeds 1 Crab. The source is a member of a high-mass X-ray binary system with a companion star (BQ Cam) that belongs to the class of *Be* stars. According to current ideas (e.g. Okazaki & Negueruela 2001), such objects represent quick rotating stars with a dense, but radially slow, stellar wind. This wind forms the so-called equatorial disc around the star, the size and the presence of the disc are not permanent. Most X-ray sources in binary systems with *Be* stars are transients demonstrating outbursting activity. This is presumably connected with the evolution of the normal star. Matter from the equatorial disc is captured, and an accretion disc around the relativistic object is formed.

The system V0332+53/BQ Cam is an obvious example of the picture described above. As was shown by Goranskij (2001), a significant brightening of the normal star in the optical waveband preceded previous X-ray outbursts. It is believed that this brightening

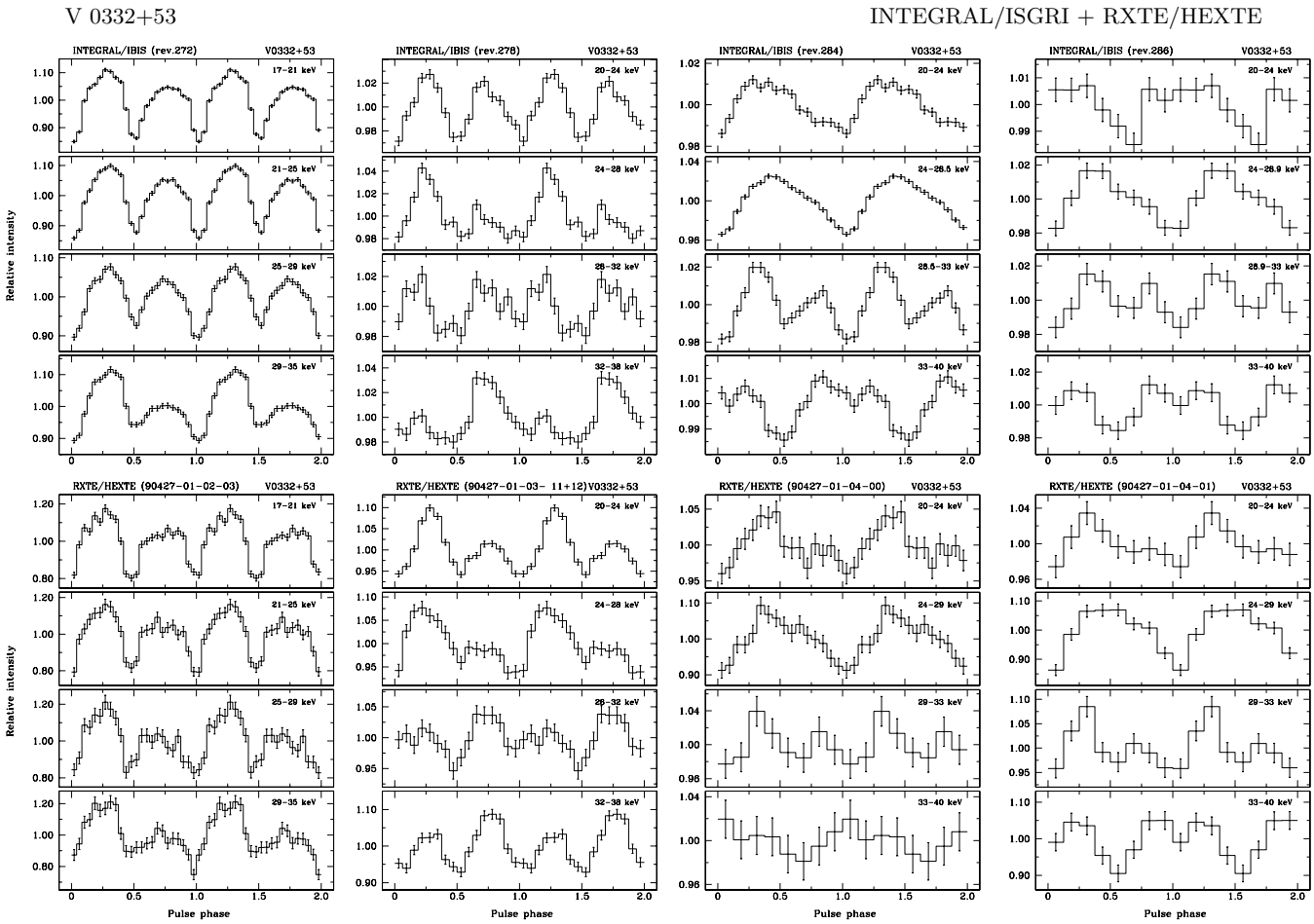

Figure 7. Evolution of the source pulse profile near the cyclotron line with the source intensity. IBIS/*INTEGRAL* data (upper panels) and HEXTE/*RXTE* data (bottom panels). The pulse phase zero for each observation is chosen independently.

is associated with the formation and subsequent ejection of the ambient matter (equatorial disc; Goranskij 2001). The outburst that started in 2004 December was no exception and had been predicted on the basis of an increase in the brightness of the optical star at the beginning of 2004 (Goranskij & Barsukova 2004). Such a huge (several hundred days) delay between the optical and X-ray light is typical for this source (Goranskij 2001) and is possibly associated with the necessity to accumulate in the accretion disc the sufficient amount of matter to begin accretion. The idea that accretion during outbursts proceeds through the disc is supported by the high observed luminosity ($\sim 5 \times 10^{38}$ erg s^{-1}), unachievable for stellar wind accretion. Furthermore, the pulse period changes at a high rate during the outburst (Tsygankov et al., in preparation), which is typical for binary systems with disc accretion and is observed in other transient X-ray pulsars with *Be* companions [see e.g. Tsygankov & Lutovinov (2005) for KS1947+300].

6.1 Cyclotron line

It was found by Basko & Sunyaev (1976a) that there is a critical value of the luminosity ($L^* \sim 10^{37}$ erg s^{-1}) dividing two accretion regimes: the regime when the influence of the radiation on the falling matter is negligible and the regime when this influence is significant. When $L < L^*$, the matter free-fall zone is extended almost down to the surface of the neutron star. In the opposite case ($L > L^*$), observed for V0332+53, the radiation-dominated shock rises high above the neutron star surface. Almost all of the kinetic energy of the infalling gas is lost in this shock, and is then emitted laterally by the sides of the accretion column.

Basko & Sunyaev (1976a) and Lyubarskii & Sunyaev (1988) showed that the height of the shock H depends on the source luminosity

$$H \simeq \dot{m} R_{\rm NS} \ln\left(\eta \frac{1+\dot{m}}{\dot{m}^{5/4}}\right),$$

where $\dot{m}$ is the dimensionless accretion rate in units of 10^{39} erg s^{-1}, η a function depending on the magnetic field on the neutron star surface $B_{\rm NS}$ and the thickness of the accretion column. As can be seen from the equation, the height H changes practically linearly with $\dot{m}$ in a wide range of values, i.e. the shock height grows linearly when the source luminosity is increased.

It was shown above that the energy of the cyclotron line detected in the V0332+53 spectrum grows approximately linearly with decreasing source luminosity. The maximum relative change of the energy and, consequently, the corresponding magnetic field are about ~25 per cent. In an approaching dipole field of the neutron star, it corresponds to a 7.5 per cent relative change of the height h where the feature is formed. At the end of the outburst, the source luminosity falls to $\sim 10^{37}$ erg s^{-1}, the shock descends, the column height decreases and we receive emission coming virtually from the

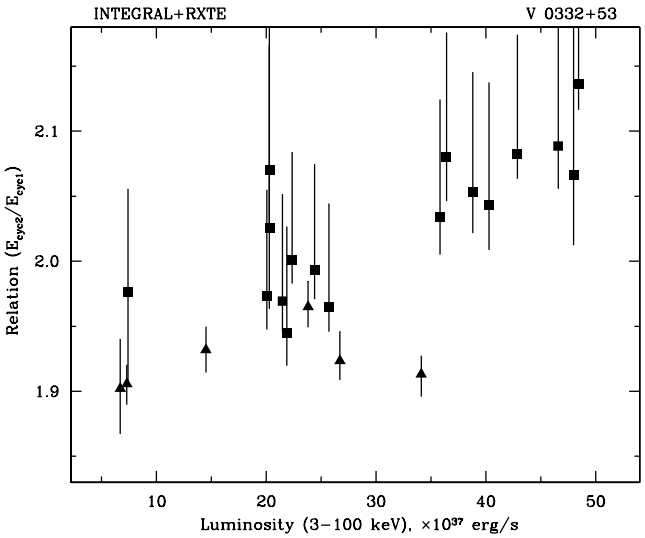

Figure 8. Dependence of the ratio of energies of second and main harmonics of the cyclotron line on the source luminosity (3–100 keV). Triangles and squares represent *INTEGRAL* and *RXTE* results, respectively.

neutron star surface. Because of the smallness of the relative change $h/R_{\rm NS}$, we can consider $B(h) \propto B_{\rm NS} - \alpha h$ to a first approximation, where α is a coefficient. Comparing with the relation between $E_{\rm cycl,1}$ and L determined earlier, we obtain $h \propto L$. Thus, the height h, where the cyclotron feature is formed, has the same luminosity behaviour as the shock height H.

According to Basko & Sunyaev (1976a), only a small fraction of the energy accumulated in the accreting matter is emitted at the shock. Its main part goes into the extended sinking zone below the shock, being gradually emitted by the sidewalls of the accreting column. Moreover, the column cross-section has a near-triangular shape where the shock properly occupies only a small part in the column central plane. In other parts, the deceleration of the infalling matter is cased by a friction force (Lyubarskii & Sunyaev 1988). Thus, the registered emission is a superposition of emissions from different heights above the neutron star surface. Therefore, we can consider the height h as some averaged or 'effective' height of the formation of the cyclotron feature not coinciding with the position of the shock itself.

As seen in Fig. 5, the behaviour of the energy of the second harmonic is qualitatively similar to the main one. But due to lower statistics of the data at high energies, the exact determination of its parameters is model-dependent (see above). Thus, at the moment we cannot make a final conclusion about the rate of change of the second harmonic energy with the source luminosity. Nevertheless, it is interesting to note that the ratio of the energies of the second and main harmonics slightly decreases with decreasing luminosity and is approximately equal to the harmonic one (2:1) near the luminosity $\sim 2 \times 10^{38}$ erg s^{-1} (Fig. 8).

6.2 Pulse profile

As experimental information about pulse profiles and their evolution has been accumulated, it has become clear that a simple model explaining pulsations by the presence of two bright spots on the neutron star surface cannot clarify the variety of observations. Our results on V0332+53 confirm this statement.

As was shown above, the matter flowing from the accretion disc forms near the magnetic poles accretion columns elongated along the magnetic lines of force. Since the falling matter is opaque, the radiation is entrained in the column and moves with the matter downwards, diffusing to the edges of the accretion channel and escaping laterally (Lyubarskii & Sunyaev 1988). Thus, a fan beam configuration of the X-ray emission is expected to prevail in the bright state (Basko & Sunyaev 1976a), which explains the observed double-peaked structure of the source pulse profile. But it is worth noting that although the radiation has time to escape from the column, it will beam towards the neutron star surface due to relativistic effects (Lyubarskii & Sunyaev 1988) and simple considerations about the beaming can be inapplicable. Most likely, the observed pulse profile variability can be explained by a combination of geometrical and physical effects. We point out some of them below.

One of the possibilities to describe the observed changes of relative intensities of peaks in the pulse profile can be the mechanism of pulse formation for large source luminosities proposed by Basko & Sunyaev (1976b). Its essence is that the magnetic field of the neutron star makes the gas to flow off to the magnetic funnels along the Alfven surface. This flow will cover only a part of the surface. The layer of matter on the surface will spin with the same angular velocity as the neutron star and will periodically shield from the observer different parts of emission regions. For a certain orientation of the system to the observer, it is possible to expect different relative intensities of peaks in a dependence on the energy band. Also, the reflection from the inner surface of the gas layer flowing to the lower magnetic field can make a contribution to the formation of the pulse profile (Basko & Sunyaev 1976b). When the source intensity is decreased, the scattering optical depth of the masking layer is also decreased, which can result in a larger amplitude of the asymmetry in the pulse profile and to an appearance of some new features in them. The calculations show that in bright states the flows on the magnetosphere are optically thick. This results in additional changes in the pulse profile, especially strong in the soft and hard energy bands (Basko & Sunyaev 1976b).

The most interesting and difficult for explanation changes occur near the main harmonic of the cyclotron line at luminosities lower than $\sim 7.3 \times 10^{37}$ erg s^{-1}. The observed behaviour is difficult to describe in detail within the framework of the current models. In part, it can be connected with peculiarities of the radiation beaming near the cyclotron frequency (Gnedin & Sunyaev 1973; Pavlov et al. 1985). For example, as shown by Meszaros & Nagel (1985), the cyclotron line shape demonstrates a strong angular dependence. The plasma is more transparent at large angles than at small ones for energies below and above the line energy. Therefore, photons will escape predominantly in the directions of large angles, i.e. the radiation beaming in different energy channels near the cyclotron line will be strongly different. In addition, a bulk motion towards the neutron star surface also produces a Doppler shift, which should result in an angular dependence of the cyclotron line energy on the viewing angle, that in its turn can give a contamination to the observed line energy and pulse profile dependencies (Brainerd & Mezaros 1991).

For the better visual perception and understanding of the changes described above, we built three-dimensional pulse profiles with the distribution of their relative intensities along the pulse phase and energy. To obtain a more or less smooth picture, we choose the energy window (the energy band for each profile) of 4 keV and reconstructed a number of pulse profiles with a step of 1 keV from 6 to 45 keV. Such an approach also allowed us to sew together JEM-X and ISGRI results around 20 keV relatively well. Two such three-dimensional pulse profiles for 272 and 284 revolutions are shown in Fig. 9 (upper panel). Both of them clearly show all of the features described in Section 5. The red and blue stripes represent regions of

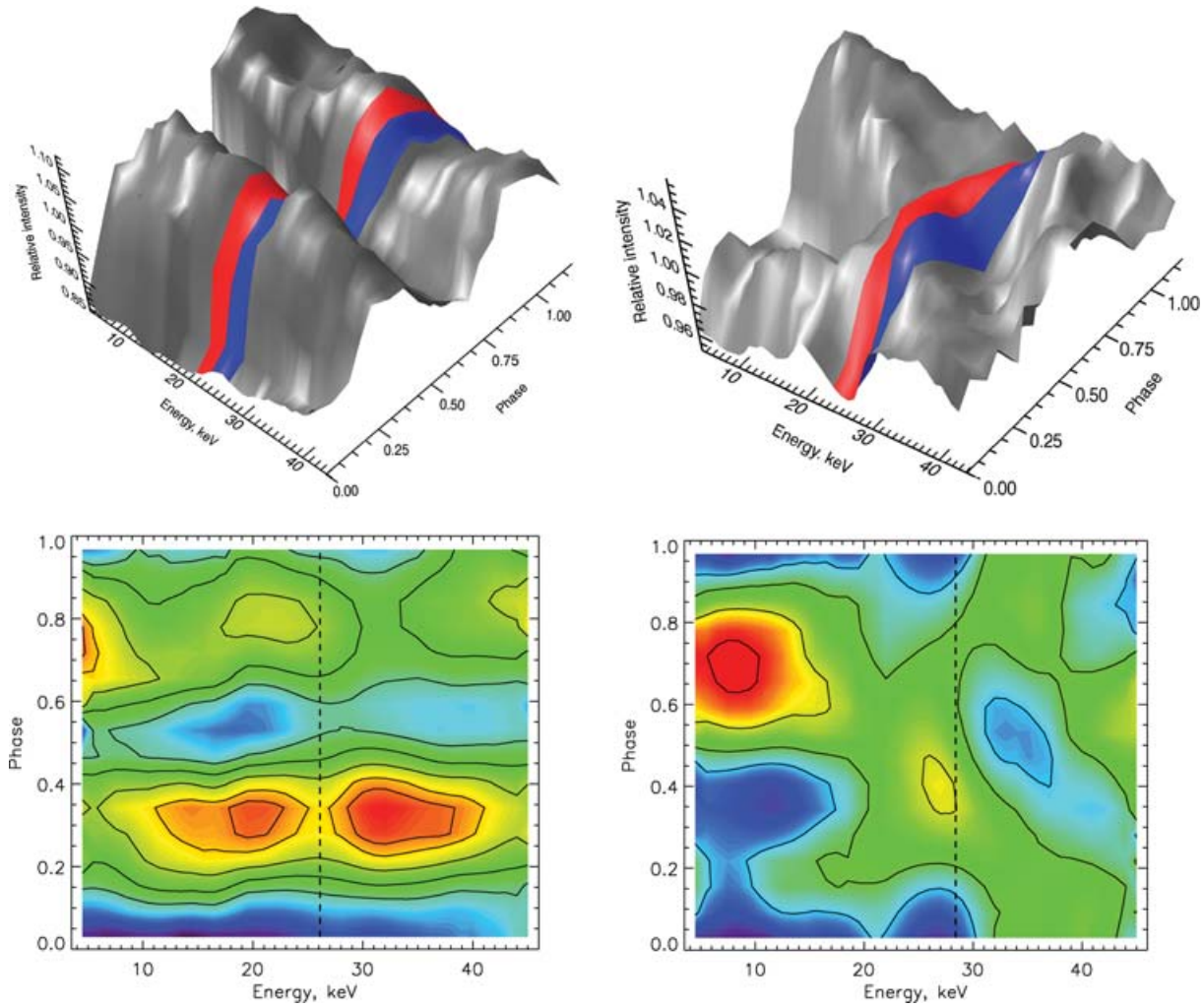

Figure 9. Three-dimensional evolution of the source pulse profiles for 272 (a) and 284 (b) revolutions. Red and blue stripes represent lower and upper wings of the cyclotron line. Two-dimensional distributions of pulse profile intensities with the energy and pulse phase are shown in the bottom panel by different colours. Solid lines represent levels of equal intensity. Positions of the cyclotron line centre are shown by dashed lines.

lower and upper wings of the cyclotron lines. In the bottom panels of Fig. 9, two-dimensional distributions of pulse profile intensities are demonstrated by different colours and levels of equal intensities. It is interesting to trace changes of the maximum intensities for both observations: in the first case, positions of both peaks are practically unchanged with the energy; in the second one, the position of the maximum is changed drastically with the energy especially near the cyclotron line. The single- and double-peaked distribution of intensities in the lower and upper wings of the cyclotron line is obviously seen.

The case of small luminosities is of special interest for following investigations. In this case, the radiating plasma have an appreciable optical depth only near the cyclotron line, and the source pulse profile reflects physical properties of the plasma flow in the magnetic field. That is, it is determined by the anisotropy of the emission and scattering in the plasma.

7 SUMMARY

We presented results of the analysis of the *INTEGRAL* and *RXTE* data obtained during the outburst from the X-ray pulsar V0332+53. The most important are as follows.

(i) For the first time, we studied in detail the evolution of the cyclotron energy with the source luminosity and showed that it is linearly increasing with the source luminosity decreasing in the same way as the change of the height of the accretion column.

(ii) The behaviour of the second harmonic energy is qualitatively similar to the main one, but more accurate observations are needed for exact measurements of its rate and understanding of the behaviour of the ratio of energies of second and first harmonics.

(iii) The strong pulse profile variations with luminosity, especially near the cyclotron line, are revealed.

ACKNOWLEDGMENTS

We thank M. Revnivtsev, R. Krivonos, M. Gilfanov and S. Sazonov for their help with the data analysis and discussion on the obtained results. We also thank the anonymous referee for useful and detailed comments. This work was supported by the Russian Foundation for Basic Research (project no. 04-02-17276), the Russian Academy of Sciences (The Origins and Evolution of Stars and Galaxies program) and grant of President of RF (NSh-1100.2006.2). AAL acknowledges financial support from the Russian Science Support Foundation. We are grateful to the European *INTEGRAL* Science

Data Centre (Versoix, Switzerland), the Russian *INTEGRAL* Science Data Center (Moscow, Russia) and the High Energy Astrophysics Science Archive Research Center Online Service, provided by the NASA/Goddard Space Flight Center, for the data. The results of this work are partially based on observations of the *INTEGRAL* observatory, an ESA project with the participation of Denmark, France, Germany, Italy, Switzerland, Spain, the Czech Republic, Poland, Russia and the United States.

REFERENCES

Basko M. M., Sunyaev R. A., 1976a, MNRAS, 175, 395
Basko M. M., Sunyaev R. A., 1976b, SvA, 20, 537
Bradt H. V., Rothschild R. E., Swank J. H., 1993, A&AS, 97, 355
Brainerd J., Mezaros P., 1991, ApJ, 369, 179
Coburn W., Kretschman P., Kreykenbohm I., McBride V. A., Rothschild R. E., Wilms J., 2005, Astron. Telegram, 381, 1
Filippova E., Tsygankov S., Lutovinov A., Sunyaev R., 2005, Astron. Lett., 31, 729
Gnedin Y., Sunyaev R., 1973, A&A, 25, 233
Goranskij V., 2001, Astron. Lett., 27, 516
Goranskij V., Barsukova E., 2004, Astron. Telegram, 245, 1
Kreykenbohm I. et al., 2005, A&A, 433, L45
Lebrun F. et al., 2003, A&A, 411, L141
Lund N. et al., 2003, A&A, 411, L231
Lyubarskii Y., Sunyaev R., 1988, Sov. Astron. Lett., 14, 390
Makishima K. et al., 1990, ApJ, 365, L59
Meszaros P., Nagel W., 1985, ApJ, 299, 138
Mihara T., Makishima K., Nagase F., 1998, Adv. Space Res., 22, 987
Mihara T., Makishima K., Ohashi T., Sakao T., Tashiro M., 1990, Nat, 346, 250
Mowlavi N. et al., 2006, A&A, 377, 161
Nakajima M., Mihara T., Makishima K., Niko H., 2006, preprint (astro-ph/0601491)
Negueruela I., Roche P., Fabregat J., Coe M. J., 1999, MNRAS, 307, 695
Okazaki A., Negueruela I., 2001, A&A, 377, 161
Pavlov G., Shibanov Y., Silant'ev N., Nagel W., 1985, ApJ, 291, 170
Pottschmidt K. et al., 2005, ApJ, 634, L97
Revnivtsev M. et al., 2004, Astron. Lett., 30, 382
Stella L., White N. E., Davelaar J., Parmar A. N., Blissett R. J., van der Klis M., 1985, ApJ, 288, L45
Stella L., White N. E., Rosner R., 1986, ApJ, 308, 669
Swank J., Remillard R., Smith E., 2004, Astron. Telegram, 349, 1
Terrell J., Priedhorsky W. C., 1973, BAAS, 15, 980
Tsygankov S., Lutovinov A., 2005, Astron. Lett., 31, 88
Winkler C., 2003, A&A, 411, L1
White N., Swank J., Holt S., 1983. ApJ, 270, 711

This paper has been typeset from a TEX/LATEX file prepared by the author.